Journal Pre-proof

Saturation mutagenesis to improve the degradation of azo dyes by versatile peroxidase and application in form of VP-coated yeast cell walls

Karla Ilić Đurđić (Conceptualization) (Investigation) (Writing - original draft), Raluca Ostafe (Methodology) (Validation), Aleksandra Đurđević Đelmaš (Methodology) (Investigation), Nikolina Popović (Validation) (Visualization), Stefan Schillberg (Writing - review and editing) (Resources), Rainer Fischer (Writing - review and editing) (Resources), Radivoje Prodanović (Conceptualization) (Supervision) (Project administration) (Writing - review and editing)

PII: S0141-0229(20)30002-8

DOI: https://doi.org/10.1016/j.enzmictec.2020.109509

Reference: EMT 109509

To appear in: *Enzyme and Microbial Technology*

Received Date: 6 October 2019

Revised Date: 25 December 2019

Accepted Date: 11 January 2020

Please cite this article as: Ilić Đurđić K, Ostafe R, Đurđević Đelmaš A, Popović N, Schillberg S, Fischer R, Prodanović R, Saturation mutagenesis to improve the degradation of azo dyes by versatile peroxidase and application in form of VP-coated yeast cell walls, *Enzyme and Microbial Technology* (2020), doi: https://doi.org/10.1016/j.enzmictec.2020.109509

Research article

Saturation mutagenesis to improve the degradation of azo dyes by versatile peroxidase and application in form of VP-coated yeast cell walls

Karla Ilić Đurđić[1], Raluca Ostafe[2,3], Aleksandra Đurđević Đelmaš[1], Nikolina Popović[1], Stefan Schillberg[4], Rainer Fischer[3,5], Radivoje Prodanović[1*]

[1]University of Belgrade-Faculty of Chemistry, Studentski trg 12-16, 11000 Belgrade, Serbia

[2]Purdue Institute of Inflammation, Immunology and Infectious Disease; Molecular Evolution, Protein Engineering and Production; Purdue University, 207 S. Martin Jischke Dr., West Lafayette, IN 47907, USA

[3]Institute of Molecular Biotechnology, RWTH Aachen University Worringerweg 1, 52074 Aachen, Germany

[4]Fraunhofer Institute for Molecular Biology and Applied Ecology IME, Forckenbeckstrasse 6, 52074 Aachen, Germany

[5]Departments of Biological Sciences and Chemistry, Purdue University, 207 S. Martin Jischke Dr., West Lafayette, IN 47907, USA

Correspondence: Prof. Radivoje Prodanović, Faculty of Chemistry, University of Belgrade, Studentski trg 12-16, 11000 Belgrade, Serbia.

E-mail: rprodano@chem.bg.ac.rs

Graphical abstract

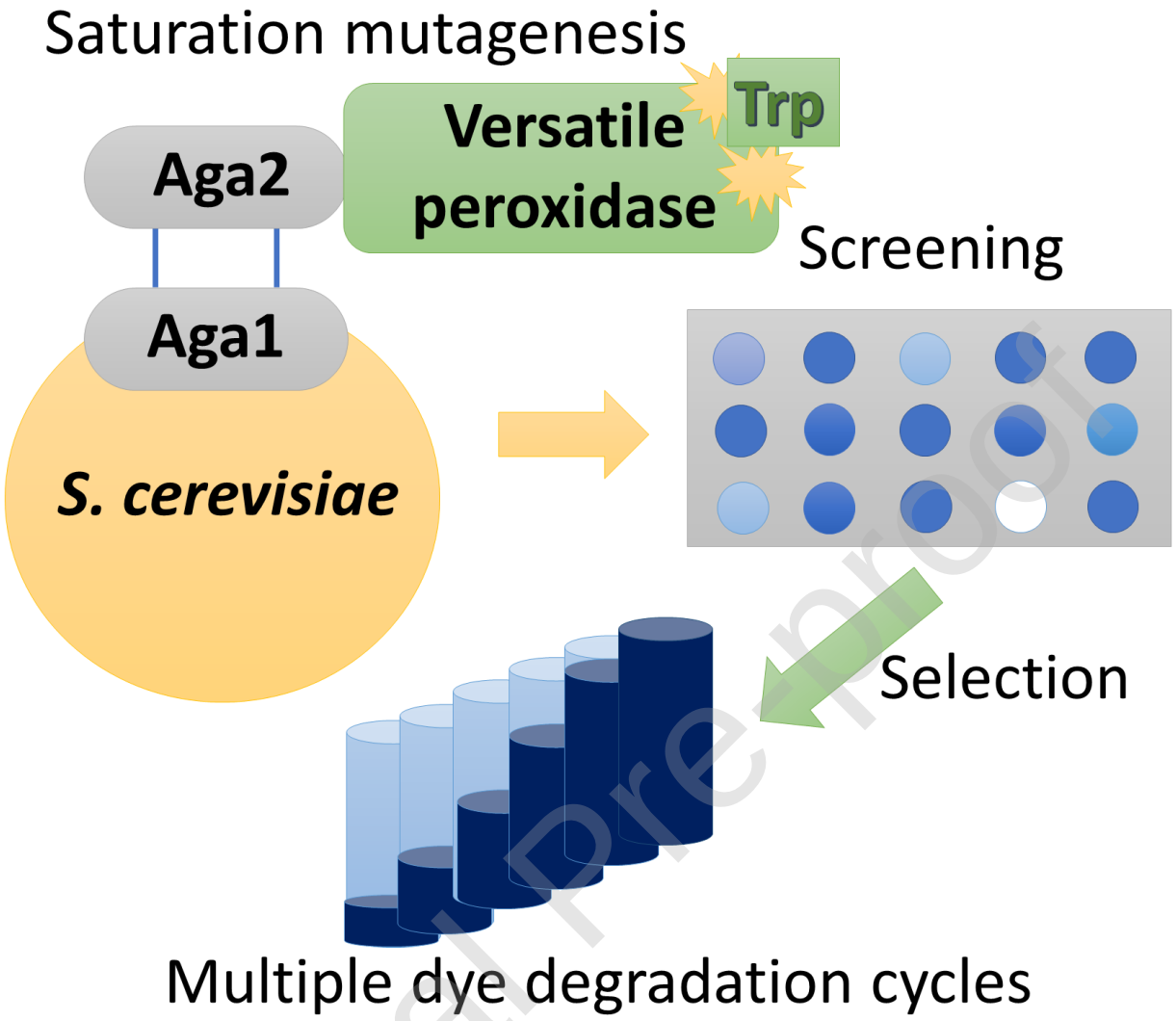

Highlights

- Azo dyes are toxic and carcinogenic synthetic pigments which accumulate as pollutants
- Versatile peroxidase is an oxidoreductase with a broad substrate spectrum
- Mutations in peroxidase catalytic Trp environment improved azo dyes degradation
- Expression on yeast cell surface and cell lysis allowed reusability of biocatalyst

ABSTRACT

Azo dyes are toxic and carcinogenic synthetic pigments that accumulate as pollutants in aquatic bodies near textile factories. The pigments are structurally diverse, and bioremediation is mostly limited to single dye compounds or related groups. Versatile peroxidase (VP) from *Pleurotus eryngii* is a heme-containing peroxidase with a broad substrate spectrum that can break down many structurally distinct pollutants, including azo dyes. The utilization of this enzyme could be facilitated by engineering to modify its catalytic activity and substrate range. We used saturation mutagenesis to alter two amino acids in the catalytic tryptophan environment of VP (V160 and A260). Library screening with three azo dyes revealed that these two positions had a significant influence on substrate specificity. We were able to isolate and sequence VP variants with up to 16-fold higher catalytic efficiency for different azo dyes. The same approach could be used to select for VP variants that catalyze the degradation of many other types of pollutants. To allow multiple cycles of dye degradation, we immobilized VP on the surface of yeast cells and used washed cell wall fragments after lysis. VP embedded in the cell wall retained ~70% of its initial activity after 10 cycles of dye degradation each lasting 12 h, making this platform ideal for the bioremediation of environments contaminated with azo dyes.

KEYWORDS

Yeast surface display, cell wall fragments, dye degradation, protein engineering, *Pleurotus eryngii*

1. INTRODUCTION

Natural dyes have been used for centuries to alter the color of textiles and materials such as paper and leather [1]. During the twentieth century, natural dyes (mostly from plants) were replaced with synthetic alternatives [2]. The textile industry now utilizes more than 7×10^5 tons of synthetic dyes and pigments every year [3]. During the coloring process, 10–15% of the dye compounds are released into wastewater, which is often discharged directly into the environment, causing pollution that can be readily observed near areas with many textile factories [4-7].

Azo dyes are one of the most common types of synthetic pigment, and most have multiple azo structures linked to phenyl and naphthyl radicals substituted with different functional groups [1]. These dyes are affordable and sustainable for industrial processes [8], but they have a negative impact on public health when they accumulate in aquatic bodies [9]. Multiple studies have shown that azo dyes released into the environment are toxic, and even carcinogenic [10-14]. Strategies to remove such dyes from water include adsorption on activated charcoal or silica gel, UV degradation, ion exchange and ozonization, but this often leads to the accumulation of degradation products that trigger secondary pollution [15,16]. Another promising strategy is biodegradation, but some of the enzymes used for this purpose achieve only partial degradation due to the complex chemical structure of the dyes [17-20]. Given the wide distribution and toxicity of azo dyes and the lack of an efficient removal system, the development of improved enzymes and new biodegradation platforms is important for both environmental preservation and public health.

Versatile peroxidase (VP) is a lignin-degrading heme-containing oxidoreductase classified as a class II peroxidase [21], which is secreted by several species of basidiomycetes, mostly from the genera *Pleurotus* and *Bjerkandera* [22,23]. In natural scenarios, VP cooperates with lignin peroxidase (LiP), manganese peroxidase (MnP) and laccase to break down lignocellulose [24,25].

VP is a hybrid enzyme that combines the catalytic characteristics of MnP (i.e., the ability to oxidase Mn^{2+} to Mn^{3+}, which when complexed by organic acids can oxidize aromatic compounds [26]) with the LiP-like ability to use the long-range electron transfer (LRET) pathway based on surface-exposed catalytic tryptophan for the oxidation of compounds with a higher redox potential [27-29]. VP can directly oxidize many high-redox-potential dyes, whereas LiP requires various redox mediators to complete the same reaction [30-32]. The main substrate for LiP is veratryl alcohol [33]. VP can also oxidize this molecule but has a much lower affinity for it [34,35]. Given the ability of VP to oxidize many aromatic, phenolic and non-phenolic substrates with wide range of redox potentials [36], including industrial dyes [37], there is significant interest in applications such as the removal of pharmaceuticals [38], pesticides [39] and humic substrates [40], the generation of new molecules [41], and cross-linking to form biomolecules [42].

Enzymes are suitable for the removal of organic pollutants from environmental matrices because they show low toxicity and are effective under mild reaction conditions [43]. The efficient and economical use of enzymes requires them to be removable and reusable, and this is generally accomplished by immobilizing them on solid matrixes such as polysaccharides [44], cross-linked aggregates [42], or porous glass beads [45]. However, this limits the activity of enzymes by restricting their diffusion, and the act of immobilization can also result in partial denaturation [46]. These issues can be overcome by using whole cells as biocatalysts [47]. Recombinant proteins can be displayed on the surface of yeast cells by expressing them as fusions to the α-agglutinin mating protein subunit 2 (Aga2). When secreted to the extracellular space, Aga2 covalently binds to another subunit (Aga1) which is anchored in the cell wall, ensuring that any recombinant protein fused to Aga2 is displayed on the yeast cell surface [48]. This approach has been used successfully to display laccase for the degradation of micropollutants [49,50].

In order to increase the activity of VP, allowing the more efficient degradation of azo dyes, we used saturation mutagenesis to exhaustively substitute two amino acid residues in the catalytic tryptophan environment, which differs in structure between VP and LiP. V160 and A260 were replaced with all other residues and the resulting library was screened for improved azo dye degradation activity. Yeast surface display was then used to produce biocatalysts in the form of cell wall fragments displaying the best-performing VP variants. These were applied in multiple cycles of dye degradation to determine the suitability of the biocatalysts for environmental remediation.

2. MATERIALS AND METHODS

2.1 Chemicals, vectors and yeast cells

All chemicals were analytical grade or higher and were purchased from Sigma-Aldrich (Taufkirchen, Germany), Applichem (Darmstadt, Germany) or Carl Roth (Karlsruhe, Germany). The pCTCON2 vector (Figure S1) and *Saccharomyces cerevisiae* EBY100 competent cells were kindly provided by Professor Dane Wittrup, Massachusetts Institute of Technology.

2.2 Cloning and transformation

A synthetic gene encoding *Pleurotus eryngii* VP was inserted into the yeast surface display vector pCTCON2 at the NheI and BamHI sites (Figure S1) to produce the recombinant vector VP-pCTCON2 (Figure S2). The sequence of the VP gene is shown in Figure S3. After ligation, the mixture was used to transform competent *Escherichia coli* XL10Gold cells (Agilent Technologies, Santa Clara, CA, USA) according to the manufacturer's instructions. Plasmid DNA was recovered using a plasmid isolation kit (Macherey-Nagel, Düren, Germany) and the integrity of the inserts was confirmed by sequencing using the primers listed in Table S1.

2.3 Preparation of VP saturation mutagenesis library

A VP saturation mutagenesis library was prepared using the QuikChange Lighting Multi Site-Directed Mutagenesis Kit (Agilent Technologies) with VP-pCTCON2 as the template and the primers listed in Table S1. The PCR mixture comprised 50 ng of template DNA, 100 ng each primer and the remaining kit components. The reaction began with a denaturation step at 95 °C for 2 min, followed by 30 cycles of denaturation at 95 °C for 20 s, annealing at 55 °C for 30 s and extension at 65 °C for 5 min, and a final extension step at 65 °C for 10 min. PCR products were digested with DpnI to remove template DNA for 10 min at 37 °C and used directly for the transformation of competent *E. coli* XL10Gold cells as above. Following the isolation of plasmid DNA as above, we sequenced 10 random clones to confirm mutagenesis.

2.4 Expression and screening of VP variants in microtiter plates

The saturation library was used to transform *S. cerevisiae* EBY100 competent cells, with the empty pCTCON2 vector as a negative control and the original VP-pCTCON2 construct as a positive control [51]. After a heat shock at 42 °C for 1 h, the cells were plated on YNB-CAA medium supplemented with 2% (w/v) glucose. Single colonies were transferred to the individual wells of 96-well plates containing 100 µL of the same medium supplemented with 50 µg/mL chloramphenicol, and the plates were incubated for 16 h at 25 °C (80% humidity), shaking at 500 rpm. We then transferred 5 µL of the cells from each well to a fresh microtiter plate containing 30 µL of the same medium per well, and incubated for another 8 h under the same conditions. We then added 100 µL of induction medium to each well (YNB-CAA medium supplemented with 2% (w/v) galactose, 50 µg/mL chloramphenicol and 500 µM 5-aminolevulinic acid) and incubated the cells for another 16 h [52].

Following the induction of VP expression, the cells were washed with 100 mM sodium tartrate (pH 3.5) and 20 µL of the suspension in each well was transferred to fresh microtiter plates containing 130 µL 100 mM sodium tartrate (pH 3.5) per well. After measuring the optical density at 600 nm (OD_{600}), we added 10 µL 10 mM H_2O_2 and 40 µL of one of the following dyes to each well: 0.1 mM Evans blue, 0.1 mM Guinea green B, or 0.1 mM Amido black 10B. The efficiency of dye degradation was determined by measuring the absorbance at 620 nm at the beginning of the reaction and after 6 h to indicate the proportion of dye remaining. For standardization, three wild-type clones were included in every microtiter plate as well as three clones transformed with the empty pCTCON2 vector. All fermentations were carried out three times (three biological replicates) and all measurements were taken in triplicate (three technical replicates). VP variants with the highest activity against one or more dyes were selected for sequencing and further characterization.

2.5 Isolation of selected VP variants

After screening in microtiter plates, yeast cells expressing the most active VP variants were inoculated into 2 mL YNB-CAA medium supplemented with 2% (w/v) glucose and 50 µg/mL chloramphenicol and cultured at 28 °C for 24 h. To isolate plasmid DNA, the cells were centrifuged (10,000 × g, 25 °C, 1 min) and the pellet was resuspended in 500 µL lysis buffer (50 mM Tris-HCl pH 7.5, 10 mM EDTA, 0.5% (v/v) 2-mercaptoethanol) containing 50 U *Arthrobacter luteus* lyticase [53]. The suspension was incubated for 2 h at 30 °C and the plasmid DNA was isolated from the lysate, sequenced and used for the retransformation of *S. cerevisiae* EBY100 cells as described above.

2.6 Yeast surface display and preparation of cell walls

Individual colonies transformed with the pCTCON2 vector, wild-type VP and selected VP variants were transferred to 20 mL YNB-CAA medium supplemented with 2% (w/v) glucose and 50 µg/mL chloramphenicol, and were cultivated at 28 °C, shaking at 160 rpm, until the OD_{600} reached 3–3.5 (~16 h). For the induction of enzyme expression, the cells were transferred to 20 mL YNB-CAA medium supplemented with 2% (w/v) galactose and 50 µg/mL chloramphenicol at OD_{600} = 0.8, and we added 20 µL 0.5 M 5-aminolevulinic acid to make a final concentration of 500 µM. The cells were incubated as above for a further 16 h then washed three times with water and resuspended in 3 mL 3% (v/v) toluene. Following cell lysis for 6 h at 25 °C, shaking at 200 rpm, the cell walls were washed ~10 times in water to remove all traces of toluene. The cell walls were then resuspended in 100 mM sodium tartrate (pH 3.5) and the OD_{600} was adjusted to 5.0.

2.7 Dye degradation

We mixed 200 µL of the cell wall preparation displaying wild-type VP or selected VP variants with 100 µL 5 mM H_2O_2, 100 µL of the dye solutions discussed above (0.5 mM final concentration in each case) and 600 µL 100 mM sodium tartrate (pH 3.5). Cell walls from yeast transformed with the empty pCTCON2 vector were prepared in the same manner and used as a negative control. For multiple cycles of dye degradation, cell walls were washed after each 12-h reaction cycle and supplied with a fresh dye/peroxide solution for a total of 10 cycles.

2.8 Extraction and purification of Aga2-VP fusion proteins from yeast cell walls

The wild-type VP and five selected variants were isolated from 500 mL culture medium by centrifugation at 3000 × g for 5 min at 4 °C, followed by resuspending the cell pellet in 50 mL 100 mM sodium acetate (pH 5.5) containing 1 mM 2-mercaptoethanol. The suspension was incubated at 4 °C for 4 h before repeating the centrifugation step [55]. The supernatant containing Aga2-VP fusion proteins was concentrated using Vivaspin ultrafiltration columns with a

molecular weight cutoff of 10 kDa (Sartorius-Stedim, Göttingen, Germany) and the concentrated supernatants were dialyzed against 20 mM sodium phosphate buffer (pH 7.4). The proteins were purified using Vivapure Q Mini H mini spin columns (Sartorius-Stedim). Fractions containing active Aga2-VP variants were collected and analyzed by denaturing sodium dodecylsulfate polyacrylamide gel electrophoresis (SDS-PAGE) in 12% gels containing 2-mercaptoethanol. Protein bands were revealed by staining with Coomassie Brilliant Blue R-250 and compared to molecular weight standards (Thermo Fisher Scientific, Waltham, MA, USA). Native electrophoresis was performed under the same running conditions in gels without SDS and 2-mercaptoethanol. For zymography, the gel was supplemented with 100 mM sodium tartrate (pH 3.5) containing 0.5 mM H_2O_2 and 9 mM guaiacol [55].

2.9 Characterization of enzyme properties

Kinetic constants were determined by measuring enzyme activity in different concentrations of each dye (10–100 µM) in 100 mM sodium tartrate (pH 3.5) containing 0.5 mM H_2O_2. The concentration of fusion proteins was determined by measuring the absorbance at 280 nm based on an extinction coefficient of 17585 $M^{-1}cm^{-1}$ calculated using ProtParam.

3. RESULTS AND DISCUSSION

The wild-type VP gene was inserted into the yeast surface display vector pCTCON2 and saturation mutagenesis was carried out at positions V160 and A260. The resulting VP variants were expressed as a library of Aga2 fusion proteins, allowing them to be displayed on the yeast cell surface by binding to Aga1. Colonies expressing VP variants were screened in microtiter plates for their ability to degrade azo dyes, and the best-performing variants were sequenced, extracted from the yeast cell surface, purified, and used for further characterization. Following cell lysis and washing, the cell walls were used for multiple rounds of dye degradation (Figure 1).

3.1 Selection of residues for saturation mutagenesis

The mutation sites were selected based on differences between VP and LiP in the environment of the catalytic tryptophan, which is located at position 171 in LiP and 164 in VP (Figure 2). Trp171 in LiP is surrounded by four acidic residues (E168, E250, D165 and D264), whereas Trp164 in VP is surrounded by two acidic residues (E161 and E243), one basic residue (R257), and one neutral residue (S158). The conserved acidic residues may help to stabilize the cation radical formed on Trp during the catalytic cycle of both enzymes [31]. The replacement of R257 with an acidic residue was previously shown to cause the complete loss of VP activity against high-redox-potential dyes [34]. Another major difference concerns the surface of the Trp region, which features two bulky amino acids in LiP (L167 and F267) but two small residues in VP (V160 and A260). These residues may be responsible for the different substrate preferences of the two enzymes [31]. When the alanine at position 260 in VP was changed to phenylalanine, the equivalent residue in LiP, the kcat and Km values of the A260F enzyme variant for the common azo dye Reactive black 5 (RB5) were lower than the wild-type values, but the catalytic efficiency was unaffected, confirming that the residue at position 260 influences the substrate specificity of VP [34]. All mutations introduced around catalytic Trp164 affected the kinetic parameters of VP for different substrates [31, 34]. The valine residue at position 160 is in close proximity to Trp164 and is not conserved among peroxidases having different specificities (Figure S4). The effect of position 160 on VP substrate specificity was also indicated, but not experimentally tested by Ruiz-Dueñas et al. [34]. Therefore, in order to improve the degradation of azo dyes by VP, we selected the positions V160 and A260 for saturation mutagenesis.

3.2 Preparation and screening of the saturation mutagenesis library

A saturation mutagenesis library at positions 160 and 260 was prepared using the QuikChange Lighting Multi Site-Directed Mutagenesis Kit, and success was confirmed by sequencing 10 randomly picked clones. All 10 clones featured a mutation at one or both sites, but no mutations were detected at other positions. We obtained ~10^4 bacterial transformants, and following plasmid recovery and yeast transformation, we obtained a saturation library pool of 2×10^3 VP variants in microtiter plates (normalized to OD_{600} = 1) for the screening of azo dye degradation activity. We tested three dyes: Evans blue, Guinea green B, and Amido black 10B (Figure S5).

The proportion of cells expressing VP variants that were inactive, less active, equally active or more active compared to wild-type VP differed according to the dye (Figure 3). The proportion of cells expressing more-active VP variants ranged from 4% (against Guinea green B) to 15% (against Evans blue), with 10% of variants showing greater than wild-type activity against Amido black 10B.

The diversity evident in these activity charts indicated that the mutation sites had a significant influence on the substrate specificity of VP, but there was still a relatively high proportion of variants with equivalent activity to the wild-type enzyme (24–35%), probably reflecting the presence of variants with structurally-similar replacement residues. Given the major structural differences between the three substrate dyes, we anticipated different activity profiles [19], especially where changes in specificity were driven by differences in substrate-binding capacity.

3.3 Dye degradation by VP and its variants embedded in the yeast cell wall

Yeast cells displaying VP variants with the highest activities against one or more of the test dyes (Table 1) were regrown and the plasmids were isolated, introduced into *E. coli* XL10Gold cells for multiplication, isolated for sequencing, and then used for the retransformation of yeast.

Sequencing showed diversity in both the size and charge of amino acids present at the selected positions, especially at position 160, which were occupied by much bulkier nonpolar amino acids.

Table 1. Amino acids at the mutation target sites in the wild-type VP and selected variants.

Variant	Position 160	Position 260
Wild-type	Val	Ala
MV1	Leu	Ser
MV2	Tyr	Ala
MV3	Tyr	Arg
MV4	Ile	Gly
MV5	Ile	Val

Following the expression of wild-type VP and the five selected variants, yeast cells were washed and lysed by toluene-induced autolysis, which was optimized by measuring the protein concentration in the supernatant and enzyme activity with ABTS as the substrate (Figures S4 and S5). The concentration of released proteins and enzyme activity increased during the first 6 h of the lysis reaction. Thereafter, the concentration of released proteins remained constant and the enzyme activity declined. The initial rise in enzyme activity was probably caused by the removal of ballast proteins from the cells, whereas the subsequent decline was likely to reflect the inactivation of VP by released proteases. Following lysis, cell walls with embedded wild-type VP or its variants were washed, resuspended in 100 mM sodium tartrate (pH 3.5) and mixed with 1 mM of the given test dye plus 0.5 mM H_2O_2. The extent of dye degradation was measured after 12 h (Figure 4).

Mutations at both positions had a significant impact on the VP-catalyzed degradation of all three azo dyes tested in this study. MV1 (Leu160, Ser260) was significantly more active against all three dyes than wild-type VP (Table 1). In contrast, MV2 and MV3 were significantly more active than the wild-type VP against Evans blue and Amido black 10B (removing 85–98% of both dyes, compared to ~40% for the wild-type enzyme), but were less active than wild-type against Guinea green B. Both of these variants feature a Tyr residue at position 160, but the residues differ at position 260 (Ala for MV2 and Arg for MV3). MV4 (Ile160, Gly260) was more active than the wild-type VP against all three dyes, but particularly against Guinea green B. Finally, MV5 (Ile160, Val260) was significantly more active than the wild-type VP against Evans blue and Guinea green, but significantly less active against Amido black 10B. As stated above, the major structural differences between the three dyes were expected to result in such differences [19].

3.4 Purification and kinetic characterization of Aga2-VP fusion proteins

The five VP variants and wild-type VP were extracted from the yeast cell wall preparation as Aga2 fusion proteins [47, 48] by incubating with 2-mercaptoethanol [55]. After buffer exchange, the extracted fusion proteins were purified by ion exchange chromatography (Figure S8) and purity was confirmed by gel electrophoresis under native conditions followed by zymography. The single bands on the native gel (Figure S9A) matched the active zones on the zymography gel with guaiacol and H_2O_2 as substrates (Figure S9B). The molecular weight of the isolated fusion proteins were determined by SDS-PAGE, revealing in each case a broad band of 50–65 kDa (Figure S10). This was higher than the theoretical molecular weight of VP (42 kDa) [23] plus Aga2 (9.5 kDa) [55], making a combined 51.5 kDa, reflecting the glycosylation that occurs during protein secretion in *S. cerevisiae* [56]. Similar results have been reported for a glucose

oxidase Aga2 fusion protein [55]. Microheterogeneity due to hyperglycosylation in *S. cerevisiae* has also been reported in the case of a secreted invertase, which showed a broad molecular weight range of 60–120 kDa [56].

Kinetic constants were determined for the VP variants against all three dyes (10–100 µM) in 100 mM sodium tartrate (pH 3.5) containing 0.5 mM H_2O_2 (Table S2). The k_{cat} and K_m values for the VP variants are compared to the wild-type enzyme in Figures 5A and 5B, respectively. For the wild-type VP fusion protein, the k_{cat} values for the three dyes fell within the range 0.81–1.17 s^{-1} and the range of K_m values was 15.76–31.28 µM. The k_{cat} of soluble wild-type VP expressed in *E. coli* for Reactive black 5 was previously reported as 5.5 s^{-1} and the K_m was 3.4 µM [34], which is consistent with our results but outside the range we observed. This may reflect the difference between the soluble enzyme and the Aga2 fusion protein, as we previously observed for glucose oxidase (wild-type and B11 mutant), where the k_{cat} value of the fusion protein was lower and the K_m value higher compared to the soluble enzyme, probably due to diffusion limitations [55].

The comparison of wild-type VP and the five selected variants revealed significant differences in k_{cat} and K_m, confirming the influence of positions 160 and 260 on these kinetic constants (Table S2). The k_{cat} value of MV1 (Leu160, Ser260) for Evans blue was 1.7-fold higher than wild-type VP whereas the K_m value was 3.5-fold lower, resulting in a significant increase in specificity. MV2 and MV3 (Tyr160) showed an even greater increase in k_{cat} compared to wild-type VP, but MV2 (Ala260) had a 4.2-fold lower K_m whereas that of MV3 (Arg260) was 1.4-fold higher. This suggests that a bulky, positively charged amino acid at position 260 is less favorable for the degradation of Evans blue. MV4 and MV5 (Ile160) had very similar kinetic parameters (slightly higher k_{cat} and significantly lower K_m than wild-type VP), but both variants featured small amino acids at position 260. Interestingly, MV1–MV4 all showed up to a 6-fold higher k_{cat} value than

wild-type VP for Amido black 10B, whereas the k_{cat} value of MV5 was 2-fold lower, suggesting that Val at position 260 has a negative impact on the degradation of Amido black 10B. MV3 showed the highest specificity constant for Amido black 10B (16-fold higher than the wild-type value). Both MV2 and MV3 (Tyr160) showed significantly lower k_{cat} values for Guinea green B compared to wild-type VP (2.5-fold and 1.5-fold lower, respectively) whereas the k_{cat} values of MV4 and MV5 (Ile160) were up to 6.3-fold higher than wild-type VP, with up to 3.8-fold lower K_m values (MV4).

Our results confirmed that both mutation sites had a significant impact on the substrate specificity of VP, and that variations at these positions affected both k_{cat} and K_m. The most significant changes were observed at position 160, where small amino acids near to the catalytic Trp residue were replaced with the much bulkier amino acids Tyr, Ile or Leu. Among the five selected mutants, both Ile and Tyr appeared twice, showing that hydrophobic and aromatic residues may promote the VP-catalyzed degradation of different dyes. Most of the amino acids identified at position 260 were small, similar to the wild-type VP, with the exception of one positively charged amino acid (Arg) in MV3. As expected, based on the negatively charged structure of the dyes, no negatively charged amino acids were identified in the selected mutants. However, the presence of negatively charged residues was confirmed in the sequences of 10 randomly chosen variants, confirming the absence of any inherent bias in the library against these residues. We also observed significant variations in the specificity of each VP variant for different dyes, confirming that the selected mutation sites are indeed important for substrate binding [31,34]. As stated above, one of the main challenges when using enzymes for the degradation of azo dyes is the diversity of dye structures [14-20], but saturation mutagenesis targeting the surface Trp environment was able to increase the catalytic efficiency of VP against all three test dyes.

3.5 Application of selected variants in multiple cycles of dye degradation

The use of enzymes for remediation is hindered by the high costs of enzyme production and their limited operational lifespan [45]. The costs can be reduced by ensuring that enzymes remain active for longer and/or by reusing them multiple times, both of which can be achieved by enzyme immobilization. However, many immobilization methods lead to the loss of enzyme activity [44-47]. We applied the strategy of *in situ* immobilization by yeast surface display and used post-lysis cell wall fragments for multiple cycles of dye degradation, in each case using the most active VP variant for each dye: MV2 for Evans blue, MV3 for Amido black 10B, and MV4 for Guinea green B (Figure 6). Each degradation cycle lasted 12 h, and the cell wall fragments were washed before the next cycle. All three selected variants lost less than 30% of their initial activity after 10 degradation cycles, proving that our biodegradation platform is ideal for remediation applications involving the removal of azo dyes.

4. CONCLUSIONS

We created a saturation mutagenesis library for two positions close to the catalytic Trp residue of VP (positions 160 and 260). In order to effectively use VP and its variants for the degradation of azo dyes, we expressed the variants on the yeast cell surface and screened the clones in microtiter plates for activity against three diverse azo dyes (Evans blue, Amido black 10B and Guinea green B). The broad range of activities we recovered confirmed that the selected mutation sites had a strong impact on the substrate specificity of VP, which may not be limited to the degradation of azo dyes. Using saturation mutagenesis, we were able to significantly improve the VP-catalyzed degradation of all three selected dyes. The five best-performing mutants differed significantly in their specificities for the three dyes, showing up to a 16-fold higher specificity than the wild-type enzyme. Sequencing revealed that hydrophobic and bulky residues at position 160 had a positive

effect on dye degradation, whereas smaller amino acids were preferred at position 260, with the exception of an Arg residue in variant MV3. The best-performing variants for each substrate were used in multiple cycles of dye degradation as cell wall fragments containing embedded enzymes. The immobilized enzymes lost less than 30% of their initial activity over 10 rounds of azo dye degradation each lasting 12 h, making them suitable for the bioremediation of contaminated aquatic bodies.

COMPETING INTEREST

The authors declare no competing financial interest.

CREDIT AUTHOR STATEMENT

Karla Ilić Đurđić: Conceptualization, Investigation and Writing original draft

Raluca Ostafe: Methodology, Validation

Aleksandra Đurđević Đelmaš: Methodology, Investigation

Nikolina Popović: Validation, Visualization

Stefan Schillberg: Writing-Review & Editing, Resources

Rainer Fischer: Writing-Review & Editing, Resources

Radivoje Prodanović: Conceptualization, Supervision, Project administration, Writing-Review & Editing

AKNOWLEDGMENTS

The authors would like to thank Professor Dane Wittrup, Massachusetts Institute of Technology, for providing the pCTCON2 vector and *S. cerevisiae* EBY100 competent cells, and Dr. Helga Schinkel, Fraunhofer IME (Aachen, Germany) for valuable discussion. This work was supported by funds from the Ministry of Education, Science and Technological Development of the Republic of Serbia via project numbers ON172049, ON173017 and III46010.

REFERENCES

1. B.C. Ventura-Camargo, M.A. Marin-Morales, Azo dyes: characterization and toxicity-A review. TLIST 2 (2013) 85-103.

2. A. Majcen-Le Marechal, Y.M. Slokar, T. Taufer, Decoloration of chlorotriazine reactive azo dyes with H2O2/UV. Dyes Pigm. 33 (1997) 281-298. https://doi.org/10.1016/S0143-7208(96)00057-5

3. P. Nigam, I.M. Banat, D. Singh, R. Marchant, Microbial process for the decolorization of textile effluent containing azo, diazo and reactive dyes. Proc. Biochem. 31 (1996) 435-442. https://doi.org/10.1016/S0960-8524(96)00113-7

4. V.M. Correia, T. Stephenson, S.J. Judd, Characterization of textile wastewaters – a review. Environ. Tech. 15 (1994) 917-929. https://doi.org/10.1080/09593339409385500

5. A. Stolz, Basic and applied aspects in the microbial degradation of azo dyes. App. Microbiol. Biotech. 56 (2001) 69-80. https://doi.org/10.1007/s002530100686

6. S. Nam, V. Renganathan, Non-enzymatic reduction of azo dyes by NADH. Chemosphere 40 (2000) 351-357. https://doi.org/10.1016/s0045-6535(99)00226-x

7. A. Jarosz-Wilkolazka, J. Kochmanska-Rdest, E. Malarczyk, W. Wardas, A. Leonowicz, Fungi and their ability to decolorize azo and anthraquinonic dyes. Enz. Microb. Tech. 30 (2002) 566-572. https://doi.org/10.1007/s12223-008-0006-1

8. S.M. Burkinshaw, A. Gotsopoulos. The pretreatment of cotton to enhance its dye ability – sulphur dyes. Dyes Pigm. 32 (1996) 209-228. https://doi.org/10.1016/S0143-7208(96)00026-5

9. W.B. Achwal. Problems during analysis of textile as per eco standards and the customer articles ordinance (Part I). Colourage 44 (1997) 29-31.

10. K.A. Amin, H. Abdel Hameid, A.H. Abdel Elsttar, Effect of food azo dyes tartrazine and carmoisine on biochemical parameters related to renal, hepatic function and oxidative stress biomarkers in young male rats. Food Chem. Toxicol. 48 (2010) 2994-2999. https://doi.org/10.1016/j.fct.2010.07.039

11. E. Idaka, T. Ogawa, H. Horitsu, Reductive metabolism of aminoazobenzenes by Pseudomonas cepacia. Bull. Environ. Contam. Toxicol. 39 (1987) 100-107. https://doi.org/10.1007/BF01691796

12. W.G. Levine, Metabolism of azo dyes: implications for detoxication and activation. Drug Metab. Rev. 23 (1991) 253-309. https://doi.org/10.3109/03602539109029761

13. F.M.D. Chequer, J.P.F. Angeli, E.R.A. Ferraz, M.S. Tsuboy, J.C. Marcarini, M.S. Mantovani, D.O. Oliveira. The azo dyes Disperse Red 1 and Disperse Orange 1 increase the micronuclei frequencies in human lymphocytes and in HepG2 cells. Mut. Res./Gen. Toxicol. Environ. Mutag. 676 (2009) 83-86. https://doi.org/10.1016/j.mrgentox.2009.04.004

14. T. Robinson, G. Mcmullan, R. Marchant, P. Nigam, Remediation of dyes in textile effluent: a critical review on current treatment technologies with a proposed alternative. Biores. Technol. 77 (2001) 247-255. https://doi.org/10.1016/S0960-8524(00)00080-8

15. J.P. Jadhav, G.K. Parshetti, S.D. Kalme, S.P. Govindwar. Decolourization of azo dye methyl red by Saccharomyces cervisiae MTCC 463. Chemosphere 68 (2007) 394-400. https://doi.org/10.1016/j.chemosphere.2006.12.087

16. I.M. Banat, P. Nigam, D. Singh, R. Marchant. Microbial decolorization of textile-dye-containing effluents: a review. Biores. Tech. 58 (1996) 217-227. https://doi.org/10.1016/S0960-8524(96)00113-7

17. K.T. Chung, J.R. Stevens. Degradation of azo dyes by environmental microorganisms and helminthes. Environ. Toxicol. Chem. 12 (1993) 2121-2132. https://doi.org/10.1002/etc.5620121120

18. S.J. Kim, M. Shoda. Decolorization of molasses and a dye by a newly isolated strain of the fungus Geotrichum candidum. Biotech. Bioeng. 62 (1999) 114-119. https://doi.org/10.1002/(SICI)1097-0290(19990105)62:1%3C114::AID-BIT13%3E3.0.CO;2-T

19. M.A. Martins, I.C. Ferreira, I.M. Santos, M.J. Queiroz, N. Lima. Biodegradation of bioaccessible textile azo dyes by Phanerochaete chrysosporium. J. Biotech. 89. (2001) 91-98. https://doi.org/10.1016/S0168-1656(01)00318-2

20. R.G. Saratale, G.D. Saratale, J.S. Chang, S.P. Govindwar, Bacterial decolorization and degradation of azo dyes: A review. J. Tai. I. Chem. Eng. 42 (2011) 138-157. https://doi.org/10.1016/j.jtice.2010.06.006

21. A.T. Smith, N.C. Veitch, Substrate binding and catalysis in hem peroxidases. Curr. Opin. Chem. Biol. 2 (1998) 269-278. https://doi.org/10.1016/S1367-5931(98)80069-0

22. T. Mester, J.A. Field, Characterization of a novel manganese peroxidase-lignin peroxidase hybrid isozyme produced by Bjerkandera species strain BOS55 in the absence of manganese. J. Biol. Chem. 273 (1998) 15412-15417. https://doi.org/10.1074/jbc.273.25.15412

23. F.J. Ruiz-Dueñas, M.J. Martínez, A.T. Martínez. Molecular characterization of a novel peroxidase isolated from the ligninolytic fungus Pleurotus eryngii. Mol. Microbiol. 31 (1999) 223-235. https://doi.org/10.1046/j.1365-2958.1999.01164.x

24. T.K. Kirk, R.L. Farrell. Enzymatic "combustion": The microbial degradation of lignin. Annu. Rev. Microbiol. 41 (1987) 465-505. http://dx.doi.org/10.1146/annurev.mi.41.100187.002341

25. F.J. Ruiz-Dueñas, A.T. Martínez. Microbial degradation of lignin: how a bulky recalcitrant polymer is efficiently recycled in nature how we can take advantage of this. Microb. Biotechnol. 2 (2009) 164-177. https://doi.org/10.1111/j.1751-7915.2008.00078.x

26. F.J. Ruiz-Dueñas, M. Morales, M. Pérez-Boada, T. Choinowski, M.J. Martínez, K. Piontek, A.T. Martínez, Manganese oxidation site in Pleurotus eryngii versatile peroxidase: A site-directed mutagenesis, kinetic and crystallographic study. Biochemistry 46 (2007) 66-77. https://doi.org/10.1021/bi061542h

27. W.A. Doyle, W. Blodig, N.C. Veitch, K. Piontek, A.T. Smith. Two substrate interaction sites in lignin peroxidase revealed by site-directed mutagenesis. Biochemistry 37 (1998) 15097-15105. https://doi.org/10.1021/bi981633h

28. M. Ayala-Aceves, M.C. Baratto, Basosi R, Vázquez-Duhalt R, Pogni R. Spectroscopic characterization of a manganese–lignin peroxidase hybrid isozyme produced by Bjerkandera adusta in the absence of manganese: evidence of a protein-centred radical by hydrogen peroxide. J. Mol. Cat. B: Enzym. 16 (2001)159–167. https://doi.org/10.1016/S1381-1177(01)00056-X

29. Y.X. Wang, R. Vázquez-Duhalt, M.A. Pickard. Manganese-lignin peroxidase hybrid from Bjerkandera adusta oxidizes polycyclic aromatic hydrocarbons more actively in the absence of manganese. Can. J. Microbiol. 49 (2003) 675-682. https://doi.org/10.1139/w03-091

30. P.J. Harvey, H.E. Schoemaker, J.M. Palmer, Veratryl alcohol as a mediator and the role of radical cations in lignin biodegradation by Phanerochaete chrysosporium. FEBS Lett. 195 (1986) 242-246. https://doi.org/10.1016/0014-5793(86)80168-5

31. Pérez-Boada M, Ruiz-Dueñas FJ, Pogni R, Basosi R, Choinowski T, Martínez MJ, Piontek K, Martínez AT. Versatile peroxidase oxidation of high redox potential aromatic compounds: site-directed mutagenesis, spectroscopic and crystallographic investigations of three long-range electron transfer pathways. J. Mol. Biol. 354 (2005) 385–402. https://doi.org/10.1016/j.jmb.2005.09.047

32. R. Tinoco, J. Verdín, R. Vázquez-Duhalt, Role of oxidizing mediators and tryptophan 172 in the decoloration of industrial dyes by the versatile peroxidase from Bjerkandera adusta. J. Mol. Catal. B: Enzym. 46 (2007) 1-7. https://doi.org/10.1016/j.molcatb.2007.01.006

33. A. Khindaria, I. Yamazaki, S.D. Aust, Stabilization of the veratryl alcohol cation radical by lignin peroxidase. Biochemistry 35 (1996) 6418-6424. https://doi.org/10.1021/bi9601666

34 F.J. Ruiz-Dueñas, M. Morales, M.J. Mate, A. Romeo, M.J. Martínez, A.T. Smith, A.T. Martínez. Site-directed mutagenesis of the catalytic tryptophan environment in Pleurotus eryngii versatile peroxidase. Biochemistry 47 (2008) 1685-1695. https://doi.org/10.1021/bi7020298

35. H. Kamitsuji, T. Watanabe, Y. Honda, M. Kuwahara. Direct oxidation of polymeric substrates by multifunctional manganese peroxidase isozyme from Pleurotus ostreatus without redox mediators. Biochem. J. 386 (2005) 387-393. https://doi.org/10.1042/BJ20040968

36. E. Rodríguez, O. Nuero, F. Guillén, A.T. Martínez, M.J. Martínez. Degradation of phenolic and non-phenolic aromatic pollutants by four Pleurotus species: the role of laccase and versatile peroxidase. Soil Biol. Biochem. 36 (2004) 909–916. https://doi.org/10.1016/j.soilbio.2004.02.005

37. M. Hibi, S. Hatahira, M. Nakatani, K. Yokozeki, S. Shmizu, J. Ogawa, Extracellular oxidases of Cerrena sp. complementary functioning in artificial dye decolorization including laccase, manganese peroxidase, and novel versatile peroxidases. Biocat. Agricul. Biotech. 1 (2012) 220-225. https://doi.org/10.1016/j.bcab.2012.03.003

38. I.E. Touahar, L. Haroune, S. Ba, J.P. Bellenger, H. Cabana, Characterization of combined cross-linked enzyme aggregates from laccase, versatile peroxidase and glucose oxidase, and their utilization for the elimination of pharmaceuticals. Sci. Tot. Environ. 481 (2014) 90-99. https://doi.org/10.1016/j.scitotenv.2014.01.132

39. G. Davila-Vazquez, R. Tinoco, M.A. Pickard, R. Vazquez-Duhalt, Transformation of halogenated pesticides by versatile peroxidase from Bjerkandera adusta. Enz. Microb. Tech. 36 (2005) 223-231. https://doi.org/10.1016/j.enzmictec.2004.07.015

40 K.S. Siddiqui, H. Ertan, T. Charlton, A. Poljak, A.K.D. Khaled, X. Yang, G. Marshall, R. Cavicchioli, Versatile peroxidase degradation of humic substrates: Use of isothermal titration calorimetry to assess kinetics, and applications to industrial waste. J. Biotech. 178 (2014) 1-11. https://doi.org/10.1111/j.1751-7915.2008.00078.x

41. E. de Jong, J.A. Field, J.A.F.M. Dings, J.B.P.A. Wijnberg, J.A.M. de Bont. De novo biosynthesis of chlorinated aromatics by the white-rot fungus Bjerkandera sp BOS55. Formation of 3-chloro-anisaldehyde from glucose. FEBS Lett. 305 (1992) 220-224. https://doi.org/10.1016/0014-5793(92)80672-4

42. D. Salvachúa, A. Prieto, M.L. Mattinen, T. Tamminen, T. Liitiä, M. Lille, S. Willför, A.T. Martínez, M.J. Martínez, C.B. Faulds. Versatile peroxidase as a valuable tool for generating new biomolecules by homogeneous and heterogeneous cross-linking. Enz. Microb. Tech. 52 (2013) 303-311. https://doi.org/10.1016/j.enzmictec.2013.03.010

43. M. Poliakoff, J.M. Fitzpatrick, T.R. Farren, P.T. Anastas. Green chemistry: science and politics of change. Science 297 (2002) 807−810. https://doi.org/10.1126/science.297.5582.807

44. O. Prodanovic, D. Spasojevic, M. Prokopijevic, K. Radotic, N. Markovic, M. Blazic, R. Prodanovic. Tyramine modified alginates via periodate oxidation for peroxidase induced hydrogel formation and immobilization. React. Funct. Polym. 93 (2015) 77-83. https://doi.org/10.1016/j.reactfunctpolym.2015.06.004

45. A. Dwevedi, A.M. Kayastha. Enzyme immobilization: a breakthrough in enzyme technology and boon to enzyme-based industries. Proteome. Res. J. 3 (2012) 333.

46. S. Datta, L.R. Christena, Y.R.S. Rajaram, Enzyme immobilization: an overview on techniques and support materials. Biotech. 3 (2013) 1−9. https://doi.org/10.1007/s13205-012-0071-7DO

47. G.M. Cherf, J.R. Cochran. Applications of yeast surface display for protein engineering. Methods Mol. Biol. 1319 (2015) 155-175. https://doi.org/10.1007/978-1-4939-2748-7_8DO

48. S.A. Gai, K.D. Wittrup. Yeast surface display for protein engineering and characterization. Curr. Oppin. Struct. Biol. 17 (2007) 467-473. https://doi.org/10.1016/j.sbi.2007.08.012

49.Y. Chen, B. Stemple, M. Kumar, N. Wei. Cell Surface Display Fungal Laccase as a Renewable Biocatalyst for Degradation of Persistent Micropollutants Bisphenol A and Sulfamethoxazole. Eviron. Sci. Tech. 50 (2016) 8799-8808. https://doi.org/10.1021/acs.est.6b01641

50. K. Kuroda, M. Ueda. Arming technology in yeast-novel strategy for whole-cell biocatalyst and protein engineering. Biomolecules 3 (2013) 632−650. https://doi.org/10.3390/biom3030632

51. R.D. Gietz, R.H. Schiestl, High-efficiency yeast transformation using the LiAc/SS carrier DNA/PEG method. Nat. Protoc. 2 (2007) 31-34. https://doi.org/10.1038/nprot.2007.13

52. K. Rye, S.Y. Hwang, K.H. Kim, J.H. Kang, E.K. Lee, Functionality improvement of fungal lignin peroxidase by DNA shuffling for 2,4-dichlorophenol degradability and H2O2 stability. J. Biotech. 133 (2008) 110-115. https://doi.org/10.1016/j.jbiotec.2007.09.008

53. M.V. Singh, P.A. Weil, A method for plasmid purification directly form yeast. Anal. Biochem. 307 (2002) 13-17. https://doi.org/10.1016/s0003-2697(02)00018-0

54. J.G. Lutz, J.M. Nelson, Preparation of highly active yeast invertase. J. Biol. Chem. 107 (1934) 169-177.

55. M. Blazić, G. Kovačević, O. Prodanović, R. Ostafe, M. Gavrović-Jankulović, R. Fischer, R. Prodanović, Yeast surface display for the expression, purification and characterization of wild-type and B11 mutant glucose oxidases. Prot. Expr. Pur. 89 (2013) https://doi.org/175-180. 10.1016/j.pep.2013.03.014

56. F.K. Chu, F. Maley, The effect of glucose on the synthesis and glycosylation of the polypeptide moiety of yeast external invertase, J. Biol. Chem. 255 (1980) 6392–6397.

Figure captions

Figure 1. Schematic overview of the experimental strategy. The wild-type versatile peroxidase (VP) sequence was inserted into the pCTCON2 vector to yield the VP-pCTCON2 construct, and the insert was subjected to saturation mutagenesis at two positions. The resulting library of VP variants was expressed on the surface of yeast cells and screened for azo dye degradation activity in microtiter plates (MTPs). The best-performing variants were selected for sequencing and further characterization. Cell wall fragments displaying VP were used for multiple cycles of azo dye degradation.

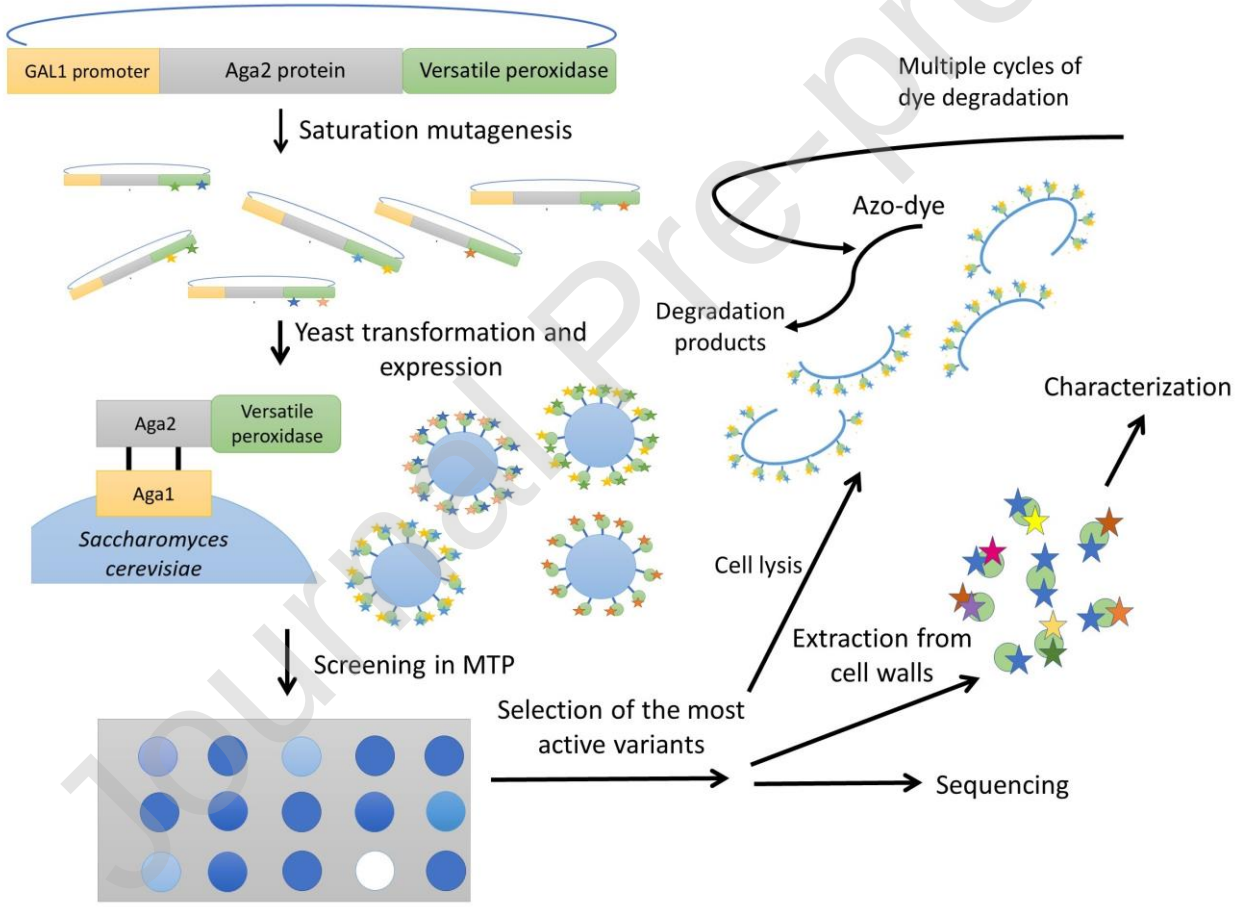

Figure 2. The catalytic tryptophan environment of versatile peroxidase (VP) and lignin peroxidase (LiP). Differences in the environment of Trp 164 for VP (A) and Trp 172 for LiP (B). Magenta residues are conserved in

both enzymes, whereas blue residues are basic or neutral in VP but acidic in LiP. Yellow residues are much bulkier in LiP than VP.

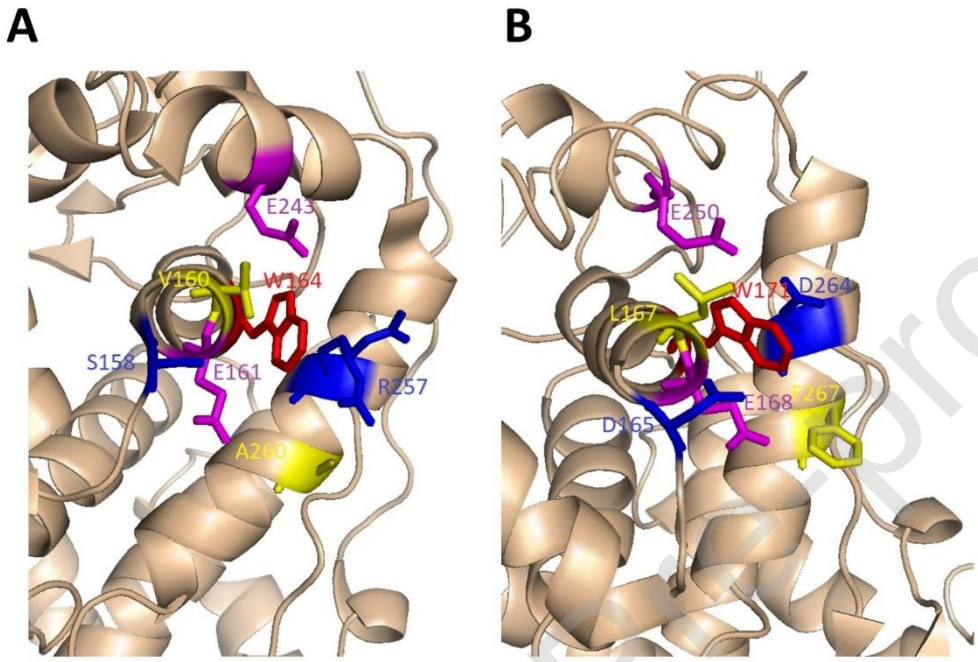

Figure 3. Proportion of versatile peroxidase (VP) variants showing no activity, lower, equal or higher activity compared to wild-type VP after screening in microtiter plates against three azo dyes: (A) Evans blue, (B) Guinea green B, and (C) Amido black 10B.

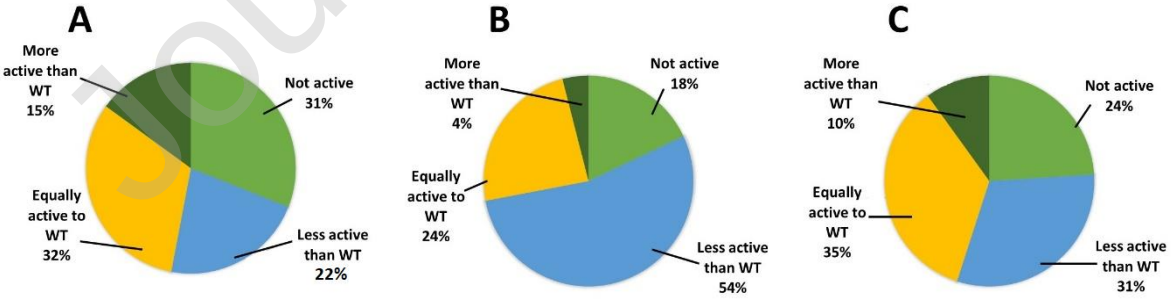

Figure 4. Dye degradation by wild-type VP and selected mutants. Following the expression of wild-type VP and selected variants, yeast cells were lysed, the cell wall fragments were washed and then mixed with three different

dyes (Evans blue, Amido black 10B, or Guinea green B, all at 1 mM) and 0.5 mM H_2O_2. The extent of dye degradation is shown as a percentage after 12 h on the y-axis, whereas the x-axis shows the wild-type VP and variants MV1–MV5). Blue = Evans blue, orange = Amido black 10B, and gray = Guinea green B. Data are means of triplicate experiments with error bars indicating standard deviations.

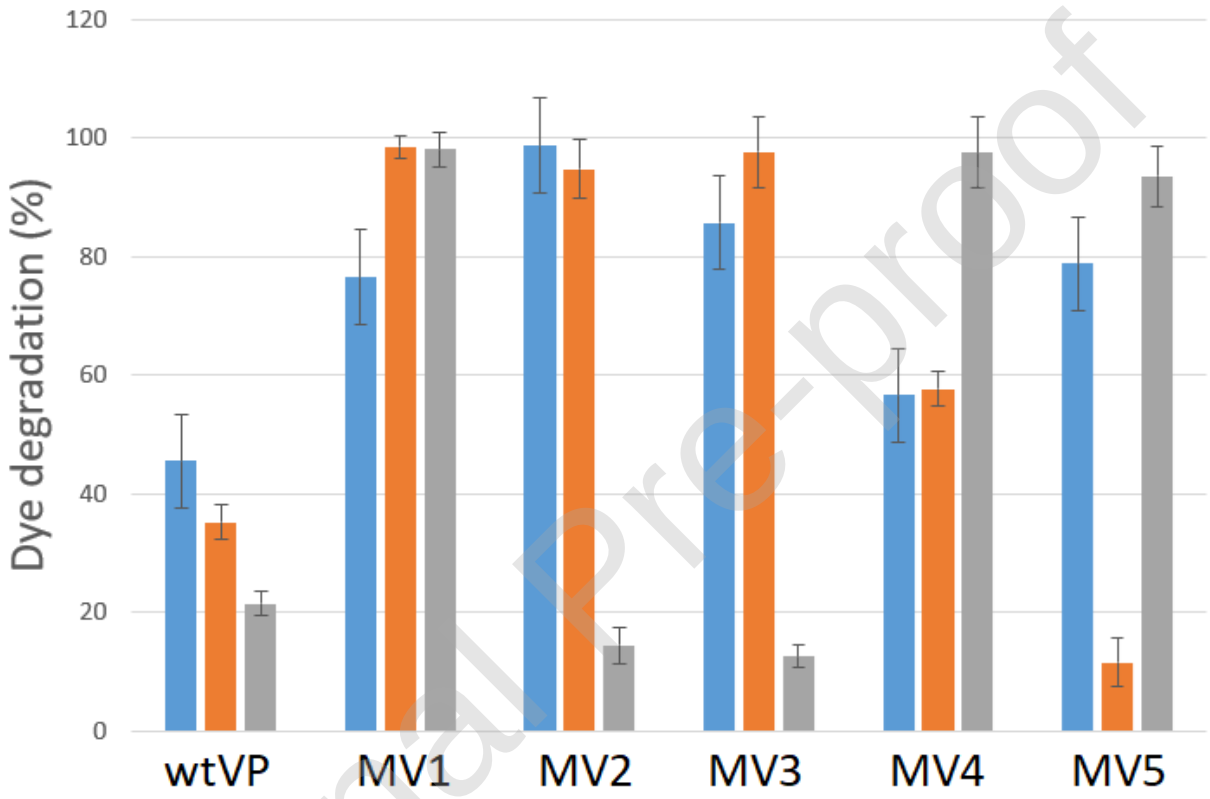

Figure 5. Kinetic parameters for wild-type VP and five selected variants. (A) Catalytic constants (k_{cat}) for wild-type VP and five selected variants for three different dyes. (B) Michaelis constants (K_m) for wild-type VP and five selected variants for three different dyes. Data are means of triplicate experiments with error bars indicating standard deviations.

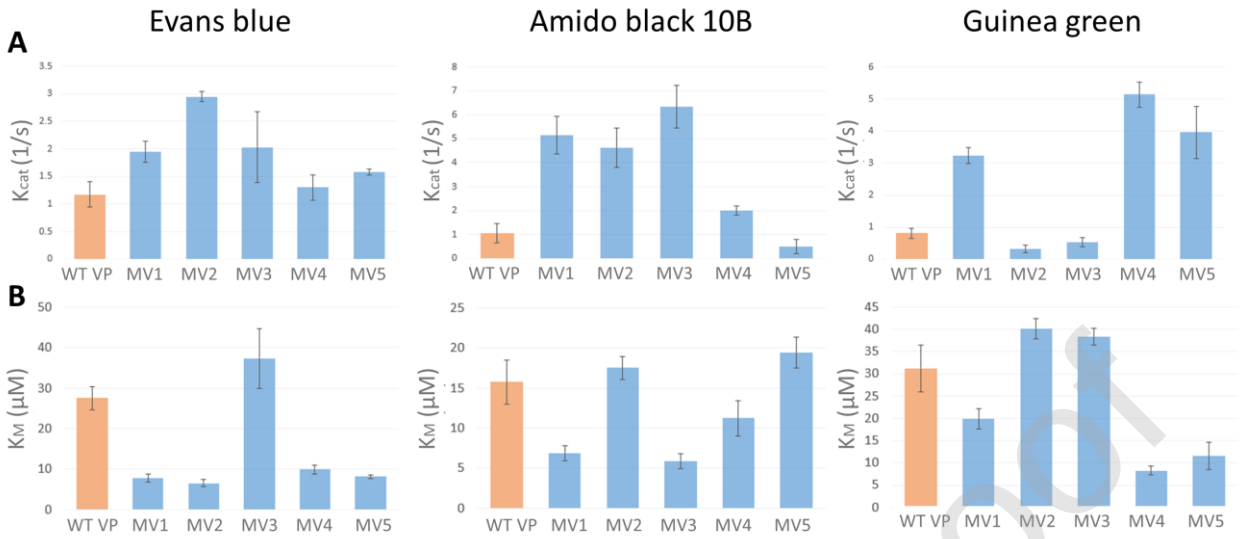

Figure 6. Multiple dye degradation cycles. (A) Evans blue degradation cycles with VP variant MV2. Cell wall fragments after lysis were incubated with 1 mM Evans blue and 0.5 mM H_2O_2 for 12 h. The incubation step was carried out for 10 cycles with intervening wash steps. (B) Guinea green B degradation cycles with VP variant MV4 under the same conditions described above. (C) Amido black 10B degradation cycles with VP variant MV3 under the same conditions described above. Data are means of triplicate experiments, with error bars indicating standard deviations. These are not visible when smaller than the symbol size.